

1

Microwave Switching Using Junction Circulators

Joseph Helszajn

Heriot Watt University, Edinburgh, UK

1.1 Microwave Switching Using Circulators

Since the direction of circulation of a circulator is determined by that of the direct magnetic field, it may be employed to switch an input signal at one port to either one or the other two. Switching is achieved by replacing the permanent magnet by an electromagnet or by latching the microwave ferrite resonator directly by embedding a current carrying wire loop within the resonator.

The schematic diagram of a switched junction is shown in Figure 1.1a. It is particularly useful in the construction of Butler-type matrices in phase array systems. A single-pole three throw version is depicted in Figure 1.1b.

Two common arrangements in which ferrite circulators may be employed to obtain microwave switching are separately illustrated in Figure 1.1c and 1.1d. The first uses a circulator in conjunction with a pin diode switch to vary the short-circuit plane terminating port 2. A transmission analog phase shifter is therefore obtained between ports 1 and 3 with this mode of operation. The second version is also a transmission configuration but now a switchable circulator is used to control the path between ports 1 and 3 of the circulator. The switching speed of the pin device is normally the faster one.

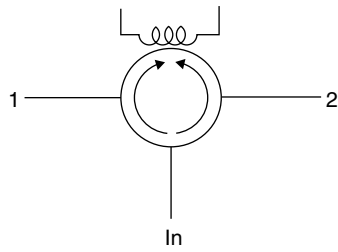
1.2 The Operation of the Switched Junction Circulator

The adjustment of a fixed field circulator or a switched circulator is a two-step procedure. The first fixes its midband frequency and the second its gyrotropy. A phenomenological description of these two operations is illustrated in

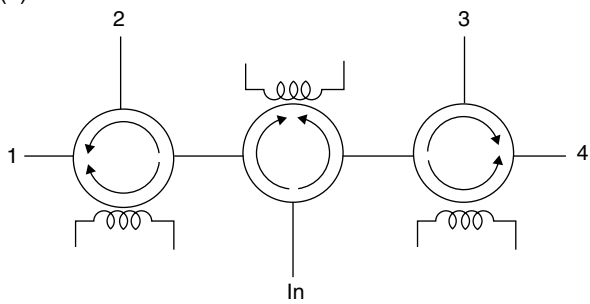
Microwave Polarizers, Power Dividers, Phase Shifters, Circulators, and Switches,
First Edition. Joseph Helszajn.
© 2019 Wiley-IEEE Press. Published 2019 by John Wiley & Sons, Inc.

2 | Microwave Polarizers, Power Dividers, Phase Shifters, Circulators, and Switches

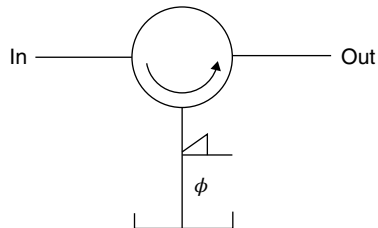
(a)



(b)



(c)



(d)

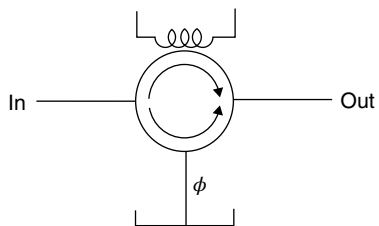


Figure 1.1 Microwave phase shifter using (a) schematic of circulator switch, (b) SP4T Butler switch using circulators, (c) pin diode switch and fixed circulator, and (d) switched circulator.

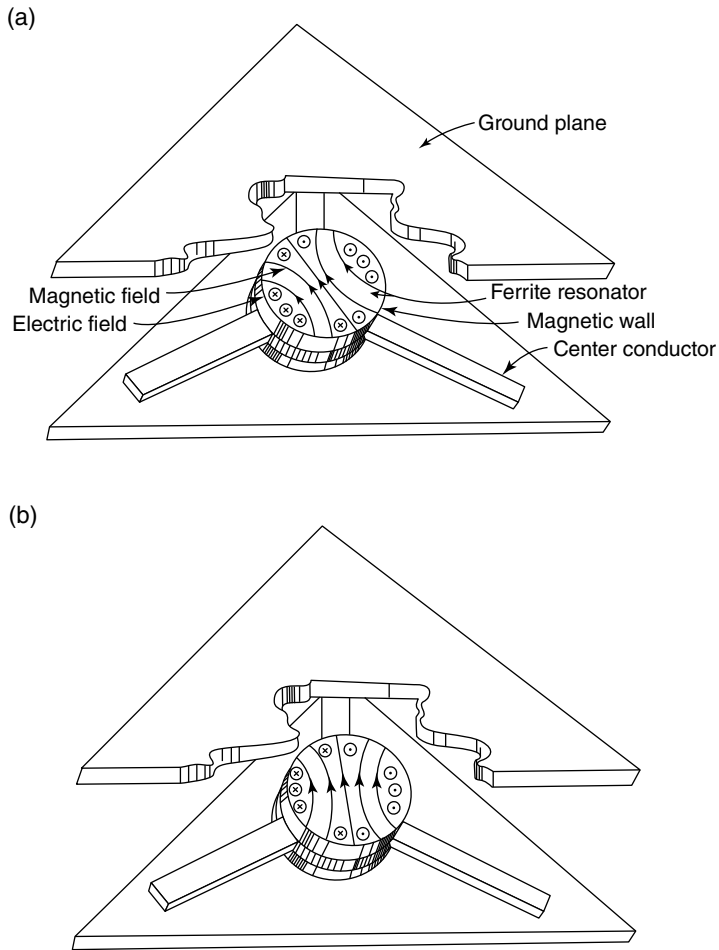


Figure 1.2 Standing wave patterns in (a) demagnetized stripline junction and (b) magnetized stripline junction.

Figure 1.2a and b in the case of a stripline geometry. The direction of circulation is here fixed by the sense of the direct magnetic field intensity along the axis of the resonator. This may be done by either internally latching the hysteresis loop of the magnetic insulator between its two remanent states or by having recourse to an external magnetic circuit. The electric field pattern may be rotated either clockwise or anticlockwise by splitting the degeneracy of the counterrotating field patterns of the resonator. A latched stripline geometry is indicated in Figure 1.3.

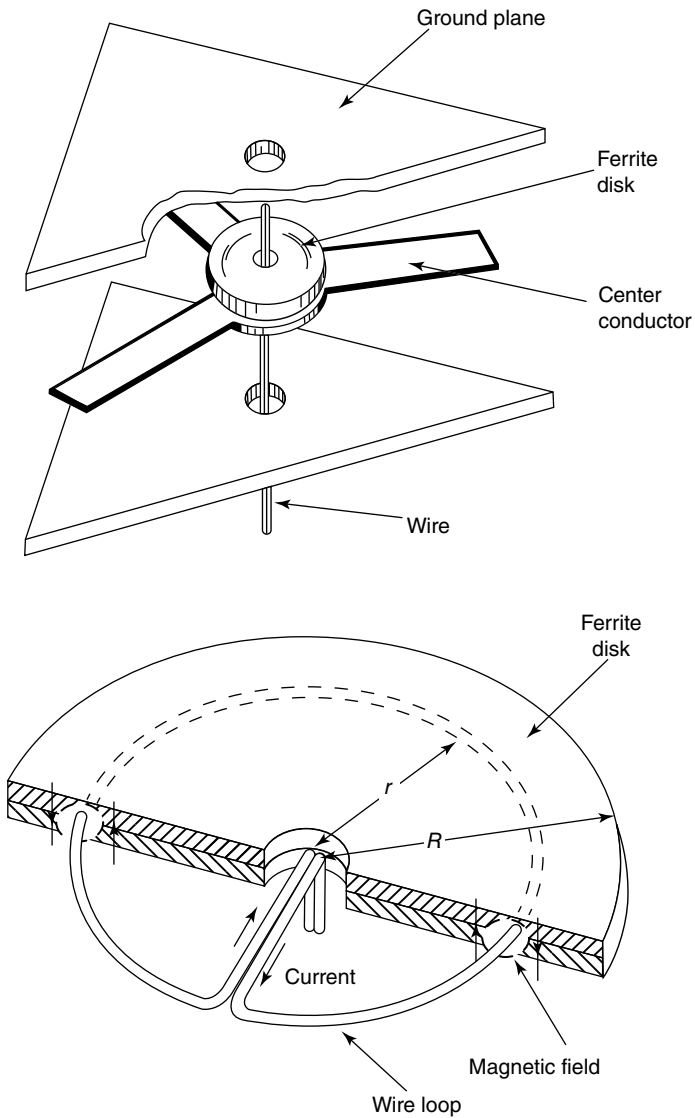


Figure 1.3 Current and magnetic field in ferrite disc.

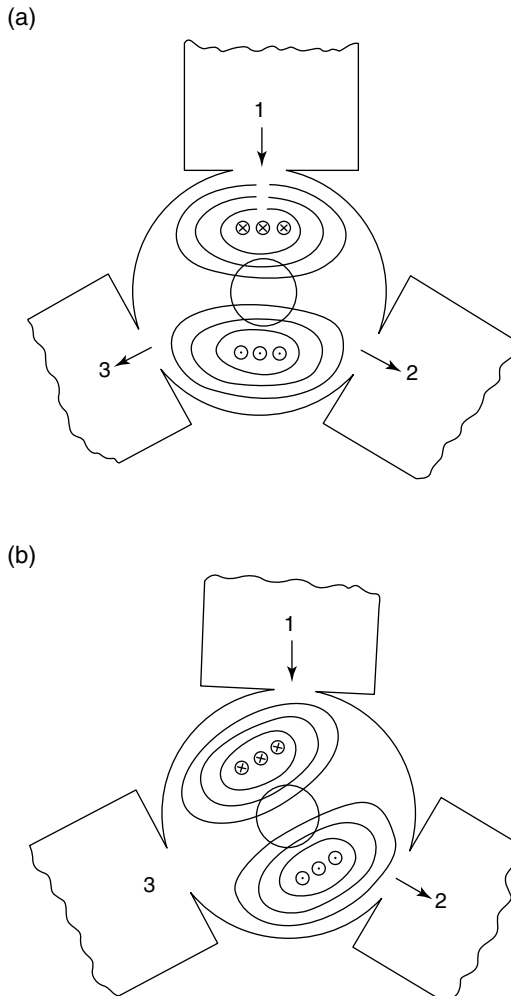
1.3 The Turnstile Circulator

The waveguide junction switch is usually but not exclusively based on a Faraday rotation effect along a quarter-wave long cavity resonator open-circuited at one flat face and short-circuited at the other. Its first circulation condition is a 90°

cavity with no rotating of the electric field pattern, which is again a figure of eight pattern. Its second circulation condition is obtained by replacing the dielectric resonator by a gyromagnetic insulator. The effect is to rotate the polarization of the electric field by a 15° angle in the positive direction of propagation and a further 15° in the opposite direction. The total rotation places an electric null at a typical output port.

Figure 1.4a and b are sketches of the electric and magnetic HE_{11} standing wave patterns about midway along the cavity. The electric field is zero at the electric wall of the cavity, whereas the magnetic field is zero at its magnetic flat wall.

Figure 1.4 (a) Ferrite unmagnetized; first circulation condition. (b) Ferrite magnetized; second circulation condition.



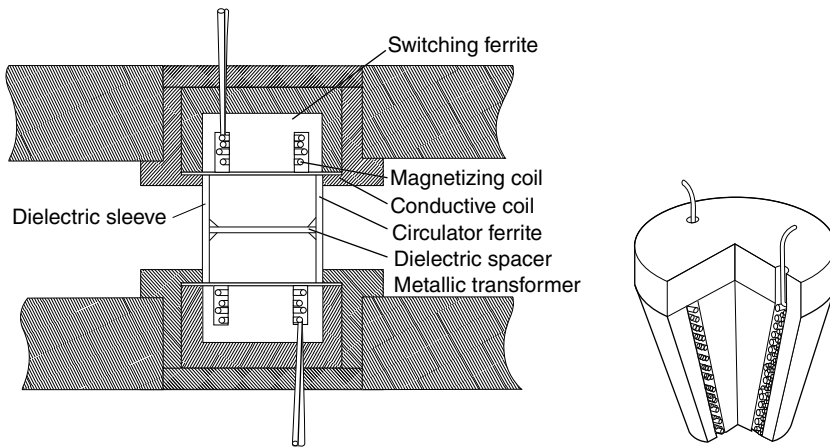
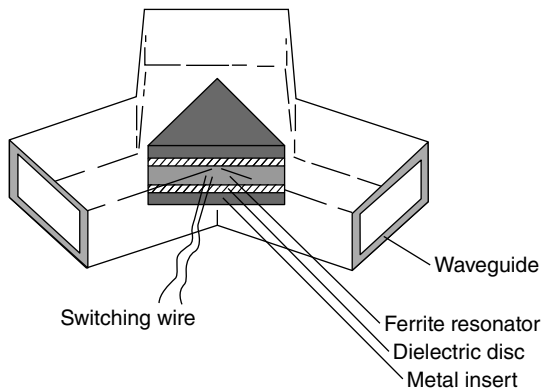


Figure 1.5 Schematic diagram of externally latched circulator using a post-resonator waveguide junction.

(a)



(b)

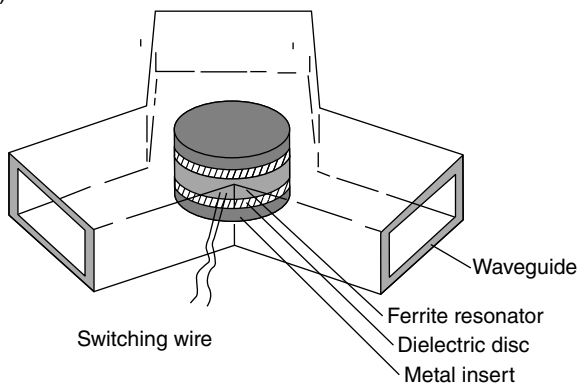


Figure 1.6 Schematic diagram of waveguide junction circulator using a partial height: (a) triangular and (b) circular resonator with a wire loop.

1.4 Externally and Internally Latched Junction Circulators

Circulators may be either actuated by an electromagnet or they may be operated by internally or externally latching the ferrite resonator. Figure 1.5 illustrates one externally latched arrangement. Figure 1.6a and b depict internally latched waveguide devices using half-wave or quarter-wave long resonators.

Figure 1.7 indicates the two possible wire configurations met in the construction of a waveguide switch using a prism resonator.

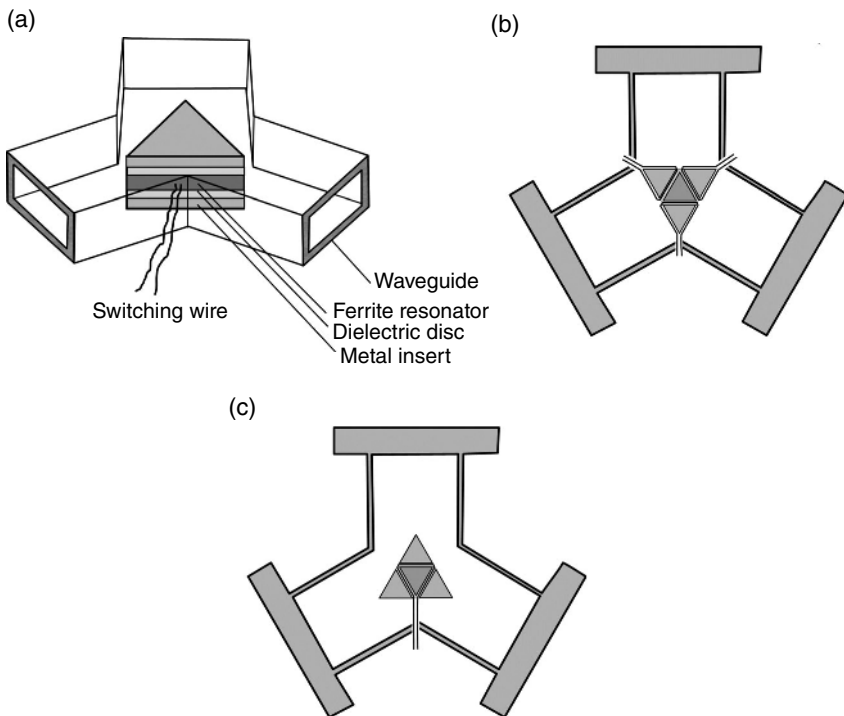


Figure 1.7 Schematic diagrams of waveguide circulators showing different switching wire configurations.

1.5 Standing Wave Solution of Resonators with Threefold Symmetry

Two resonators met in the design of switched circulators with threefold symmetry are the equilateral triangle structure and the quasi WYE geometry.

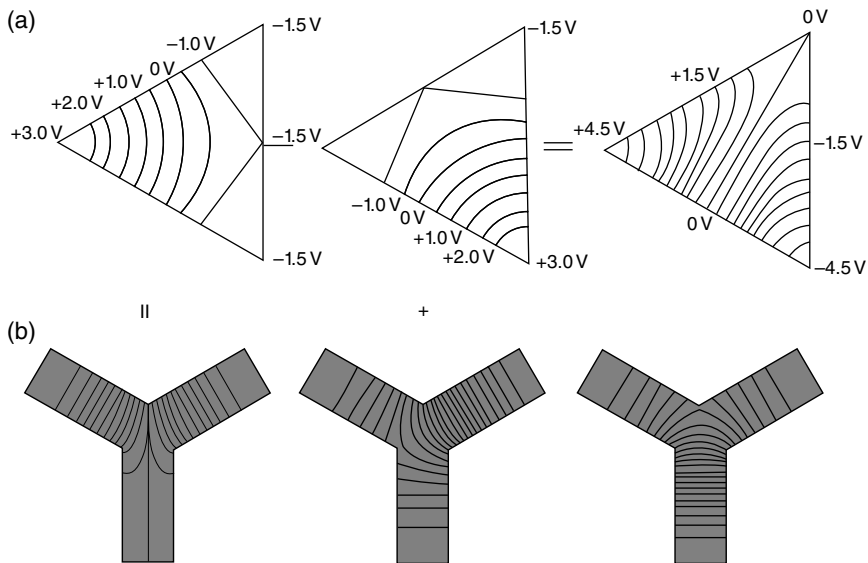


Figure 1.8 Standing wave solution of three-port circulators using (a) triangular resonator and (b) WYE resonator.

The standing wave solution of the second circulation solutions is here not obvious but each may be constructed by taking suitable linear combinations of those of the first circulation condition. Figure 1.8a and b illustrate the equipotential lines of the standing wave patterns in each situation.

1.6 Magnetic Circuit Using Major Hysteresis Loop

The direct magnetic field in a junction circulator can be established using either an external electromagnet or it can be switched by current pulses through a magnetizing wire between the two remanent states of the major or indeed of a minor hysteresis loop of a closed magnetic circuit. The former arrangement requires a holding current to hold the device in a given state.

In the latter one, however, no such current is necessary; the device remains latched in a given state until another switching operation is required. The advantages and disadvantages of each type of circuit are understood.

Operation on the major hysteresis loop may be understood by scrutinizing the hysteresis loop in Figure 1.9, providing it is recognized that the size and shape of this loop may vary with the speed of the switching process. In this situation, the magnetization of the toroid is driven between two remanent states ($\pm 4\pi M_r$)

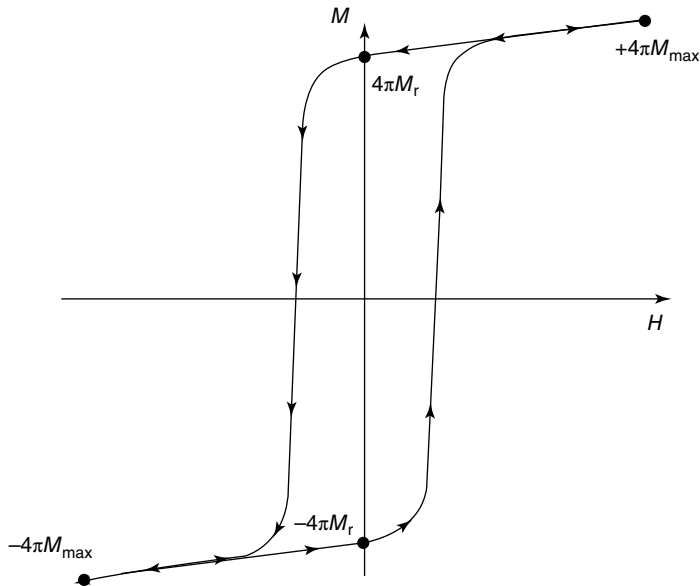


Figure 1.9 Typical hysteresis loop of a latching phase shifter operating with a major hysteresis loop switching.

equidistant from the origin by the application of a current pulse sufficiently large to produce a field perhaps three or five times that of the coercive force.

After this point is reached, the current pulse is removed and the magnetization will move to the remanent value ($\pm 4\pi M_r$) and remain there until another switching operation is desired. This sort of electronic driver circuit is relatively simple since it is only required that the toroids be driven back and forth between the major remanent states of the hysteresis loop.

1.7 Display of Hysteresis Loop

The magnetic properties and parameters of a magnetic core or toroid under different operating conditions, such as temperature, say, are best discussed in terms of the details of its hysteresis loop.

Some experimental quantities that are of particular interest include the saturation magnetization (M_0), the remanent magnetization (M_r), and the coercive force (H_c). The experimental display of such loops is therefore of some interest. One circuit that may be used for this purpose is outlined in Figure 1.10. This

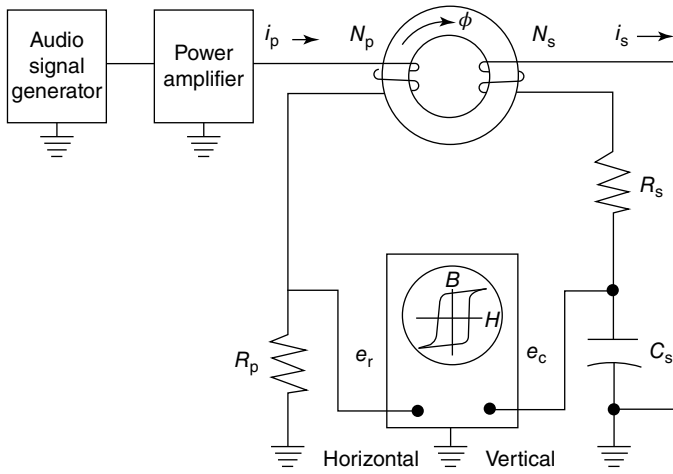


Figure 1.10 Schematic diagram of hysteresis display.

arrangement develops voltage V_p and V_i that are proportional to B and H , respectively.

The magnetic field (H) in the core is monitored by measuring the voltage (V_p) across a resistor in series with the primary winding, see Figure 1.10.

$$H = \frac{N_p}{I_p} \left(\frac{V_p}{R_p} \right), \text{A m}^{-1} \quad (1.1)$$

where I_p is the effective of the primary winding, N_p is the number of turns of the primary winding (10–30), and R_p is the resistor in series with the primary coil (10 Ω). The magnetization (B) is likewise evaluated by forming the voltage (V_i) across the capacitance of the RC integrator in the secondary circuit.

$$B \approx \frac{-V_i R_i C_i}{N_s A} \quad (1.2)$$

where R_i is the series resistance of the integrator (100 k Ω), C_i is the capacitance of the integrator (0.10 μF), N_s is the number of turns of the secondary winding (10–30), and A is the cross-sectional area of the core.

The data shown in Figure 1.11 on the effects of small air gaps on the squareness of the hysteresis loop have been obtained using the arrangement outlined here.

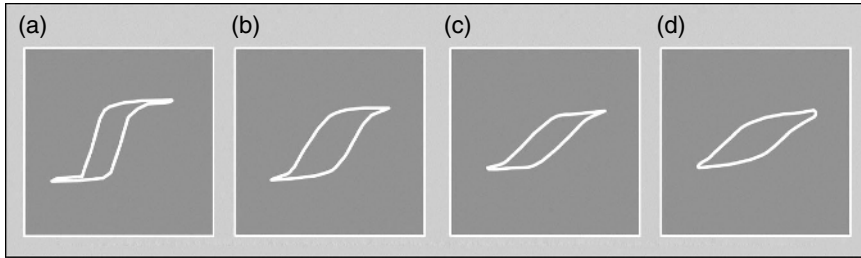


Figure 1.11 Hysteresis loops showing the effect of gaps in a magnetic circuit. (a) No gap, (b) gap of $2\frac{1}{2}$ thou, (c) gap of 5 thou, and (d) gap of 10 thou.

1.8 Switching Coefficient of Magnetization

The change of magnetization in a ferrite core consists usually in reversal of the magnetization, e.g. from negative remanence to the positive remanence corresponding to the magnetic field applied. The ultimate state of the magnetization that is set up (after the passage of the current pulse) is always symmetrical here, with respect to zero. It is observed that in most cases, the change in the magnetization produced by this field cannot follow the increase in the current.

The general situation is quite complicated but for an applied magnetic field slightly in excess of the coercive force, H_c , domain wall motion will, in general, be the predominant reversal mechanism. In this case, the flux change is accomplished by the motion of Bloch walls, which separate the domains of differently oriented magnetization.

For suitable oriented single crystals of ferrite, a very simple domain configuration may be achieved, which makes it possible to obtain information on the behavior of moving domain wall.

Studies on single crystals of ferrite have demonstrated that, under this condition, the wall velocity depends linearly on the applied magnetic field. This leads to a linear relation between the direct field and the reciprocal of the switching time. Such a relationship is also noted experimentally for polycrystalline ferrites although the actual domain configuration is not known.

The switching time is usually measured by using a core with two windings as shown in Figure 1.12. The output voltage pulse appearing at the termination of the secondary winding exhibits a characteristic shape with two separate maxima when a current pulse is passed through the magnetization winding.

For ferrite with hysteresis loops, the first maximum in the output voltage represents a small percentage of the total area under the curve and hence of the shape in magnetization.

The duration T of a voltage pulse is defined as the time (counted from the beginning of the current pulse) that elapses before the voltage has dropped

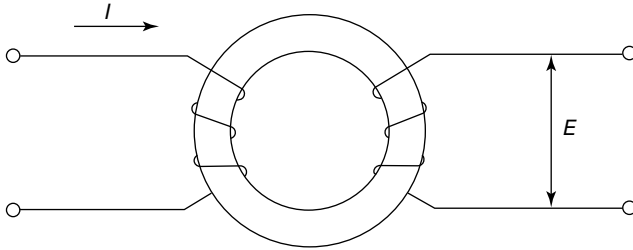


Figure 1.12 Ferrite core with two windings for measuring switching time.

to 10% of the maximum value; for the maximum value the second peak is considered. The dependence of the switching time on the magnetization producing flux reversal is most clearly represented by plotting $1/T$ as a function of the magnetizing strength H , in the manner indicated in Figure 1.13. Over the majority of the range shown, $1/T$ has a linear dependence on H , which may be adequately represented by

$$T(H - HH_0) = S \tag{1.3}$$

In this expression, S is known as the switching coefficient, and H_0 , which is of the same order of magnitude as the coercive force H_c of the material, may be termed the threshold field for irreversible magnetization. It should be noted that, although the curve is continued to values of H less than H_0 , the switching of the core under these conditions produces a smaller hysteresis loop: i.e. the material is not driven to magnetic saturation and such operation is not desirable.

The optimum squareness ratio R_s occurs for values of H fractionally different to H_0 , but it is usual to adopt magnetizing fields of between $2H_0$ and $5H_0$, the slight deterioration in squareness being accepted in the interests of faster switching.

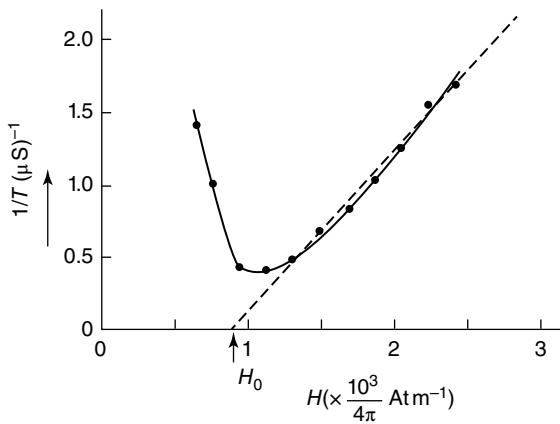


Figure 1.13 Reciprocal reversal time $1/T$ as a function of direct magnetic field H for ferroxcube. Source: Reprinted with permission Van der Heide et al. (1956).

It is found that the great majority of ferrites with the squareness and the coercive force usual for switching elements all have a reversal constant $S = (H - H_0)T$ of the same order of magnitude.

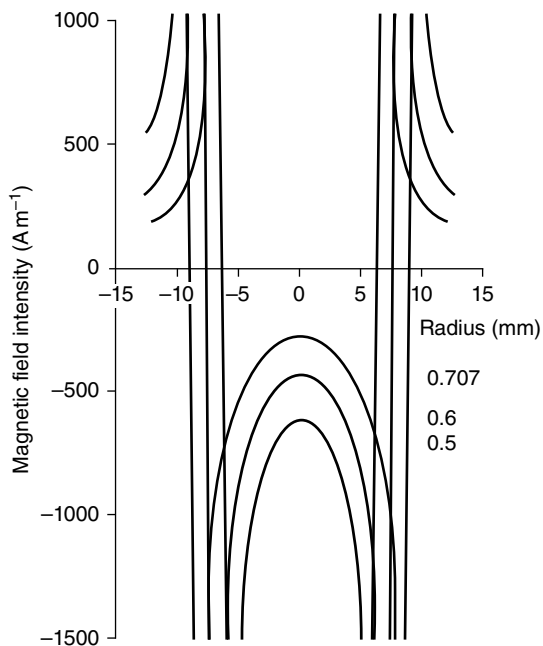
In the case of ferroxcube 6A considered above, the resultant value is $S_0 = 80 (\mu\text{s})(\text{A m}^{-1})$.

1.9 Magnetostatic Problem

One way to explore the internal direct magnetization of the magnetic insulator in the presence of one or more loops is to have recourse to a magnetostatic solver. Figure 1.14 shows the magnetizing effect of a single circular wire loop of radius r , carrying 10 A, on a cylindrical resonator with radius R . One feature of this result is that the magnetization on the axis of the loop is inversely proportional to its radius so that such switches are more readily realized at high frequencies than at lower ones.

One possible first-order model of such a resonator is one with a narrow demagnetized concentric region, a second with a magnetization in one sense, and a third with a magnetization in the other sense with still another value.

Figure 1.14 Up and down direct magnetic field strength in a cylindrical resonator using a single wire loop using a magnetostatic solver ($r/R = 0.5$, $r/R = 0.6$, $r/R = 0.707$) (Helszajn and Sharp 2012).



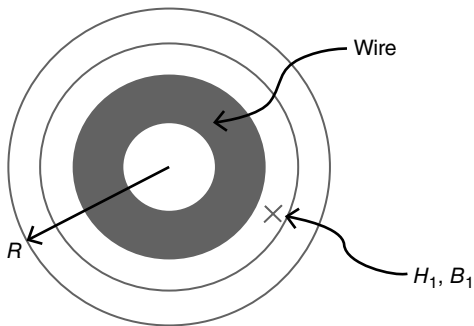


Figure 1.15 Plan view of a cylindrical resonator subdivided in concentric rings.

The more general problem divides the cross-section of the resonator into a number of concentric rings as shown in Figure 1.15.

Such a model can readily be set up, in the case of a cylindrical geometry in closed form or, in general, using a commercial FE package.

1.10 Multiwire Magnetostatic Problem

Figure 1.16 depicts the situation in the case of the pair of stacked circular loops. The spacing between the wires is half the thickness of the resonator. The inductance of the wire configuration using two wire loops is four times

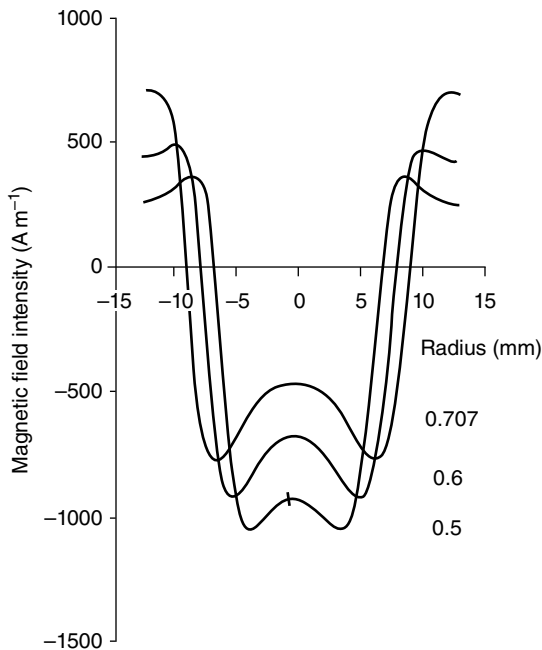


Figure 1.16 Up and down direct magnetic field strength in a cylindrical resonator using a pair of wire loops using a magnetostatic solver ($r/R = 0.5$, $r/R = 0.6$, $r/R = 0.707$) (Helszajn and Sharp 2012).

that of the single loop. The stored energy is likewise increased by a factor of four. This energy, divided by the switching time, is related to the instantaneous power required from the driver. The exact problem requires the discretization of the resonator both across and along the geometry and the assignment of the local gyrotropies in each region. This is obviously not a realistic approach without a three-dimensional solver in conjunction with a magnetostatic analyzer. It is of note, however, that the alternating magnetic field goes to zero at the open flat faces of the resonator. This means that the precise gyrotropy has no significant impact on the gyrotropy of the resonator.

1.11 Shape Factor of Cylindrical Resonator

The ratio of the two oppositely magnetized regions is defined by a shape factor q :

$$q = \frac{\text{Surface area of the inner region magnetized along the } +z \text{ direction}}{\text{Surface area of one typical outer region magnetized along the } -z \text{ direction}} \quad (1.4)$$

If the inner radius of the resonator is taken as r_i and the outer radius as r_o , then

$$q = \frac{r_i^2}{r_o^2 - r_i^2} \quad (1.5)$$

The condition $q = 1$ corresponds to that for which the cross-sectional areas of the two regions are equal.

The shape factor of a prism resonator with an equilateral core is unity. The shape factor of equilateral prism resonator employing a regular hexagonal wire is

$$q = \frac{A^2 - 3L^2}{L^2} \quad (1.6)$$

For a wye cavity with the wire loop located at the terminals between the circular region and a typical strip is

$$q = \frac{W(R-r)}{\pi r^2} \quad (1.7)$$

The work assumes a constant gyrotropy κ_{pi} in the inner region equal to 0.707 that of the saturated material, κ_o , which is taken here as 0.7. This means that the gyrotropy in the outer region lies between 0 and κ_o . When q equals unity the

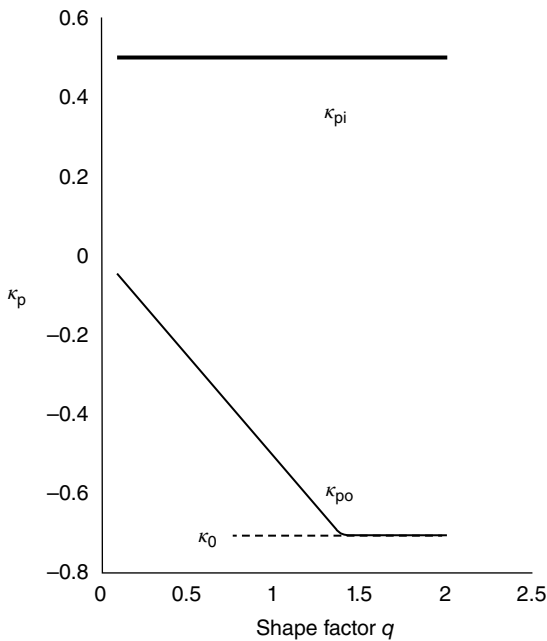


Figure 1.17 Uniform partial gyrotropy in the inner region of a composite gyromagnetic resonator against factor q (ratio of up and down surfaces) with $\kappa_{pi} = 0.5$ ($\kappa_0 = 0.7$).

partial gyrotropies in the outer region is equal to one third. The diagonal element of the tensor permeability in this work is taken as unity for simplicity sake. Figure 1.17 indicates the variation of the gyrotropy in the outer region with the shape factor q , assumed in this work.

Bibliography

- Betts, J., Temme, D.H., and Weiss, J.A. (1966). A switching circulator s-band, stripline, 15 kilowatts, 10 microseconds, temperature stable. *IRE Trans. Microw. Theory Tech.* **MTT-14**: 665–669.
- Bosma, H. (1962). On the principle of stripline circulation. *Proc. IEE* **109** (Part B, Suppl. 21): 137–146.
- Clavin, A. (1963). Reciprocal and nonreciprocal switches utilizing ferrite junction circulators. *IEEE Trans. Microw. Theory Tech.* **MTT-11**: 217–218.
- Freiberg, L. (1961). Pulse operated circulator switch. *IRE Trans. Microw. Theory Tech.* **MTT-9**: 266.
- Goodman, P.C. (1965). A latching ferrite junction circulator for phased array-switching applications. IEEE G-MTT Symposium, Clearwater, FL (5–7 May 1965). Piscataway: IEEE.

- Helszajn, J. (1960). Switching criteria for waveguide ferrite devices. *Radio Electron. Eng.* **30**: 289–296.
- Helszajn, J. and Hines, M.L. (1968). A high speed TEM junction ferrite modulator using a wire loop. *Radio Electron. Eng.* **35**: 81–82.
- Helszajn, J. and Sharp, J. (2012). Cut-off space of a gyromagnetic planar disk resonator with a triplet of stubs with up and down magnetization. *IET Microw. Antennas Propag.* **6**: 569–576.
- King, L.V. (1933). Electromagnetic shielding at radio frequencies. *Philos. Mag.* **15** (Series 7): 201.
- Laplume, J. (1945). Shielding effects of a cylindrical tube placed in a uniform magnetic field perpendicular to its axis. *Ann. Radioélectr.* **1** (1): 65–73.
- Levy, L. and Silber, L.M. (1960). A fast switching X-band circulator utilizing ferrite toroids. *WESCON/60 Conference Record*, Part 1, pp. 11–20.
- Lyons, W. (1933). Experiments on electromagnetic shielding at frequencies between one and thirty kilocycles. *Proc. IRE* **21** (4): 574–590.
- Siekanowicz, W.W. and Schilling, W.A. (1968). A new type of latching switchable ferrite junction circulator. *IEEE Trans. Microw. Theory Tech.* **MTT-16**: 177–183.
- Siekanowicz, W.W., Paglione, R.W., and Walsh, T.E. (1970). A latching ring-and-post ferrite waveguide circulator. *IEEE Trans. Microw. Theory Tech.* **MTT-18**: 212–216.
- Stern, R.A. and Ince, W.J. (1967). Design of composite magnetic circuits for temperature compensation of microwave ferrite devices. *IEEE Trans. Microw. Theory Tech.* **MTT-15**: 295–300.
- Taft, D.R. and Hodges, L.R. Jr. (1965). Square loop materials for digital phase shifter applications. *J. Appl. Phys.* **36**: 1263–1264.
- Treuhaf, M.A. and Silber, L.M. (1958). Use of microwave ferrite toroids to eliminate external magnets and reduce switching power. *Proc. IRE* **46** (8): 1538.
- Uebele, G.S. (1957). High speed ferrite microwave switch. *IRE Natl. Conv. Rec.* **5** (Part I): 227–234.
- Van der Heide, H., Bruijning, H.G., and Wijn, H.P.J. (1956). Switching time of ferrites with rectangular hysteresis loop. *Philips Tech. Rev.* **18**: 339.

